PROCEEDINGS OF SCIENCE

Cosmic-Ray Modulation during Solar Cycles 24-25 Transition Observed with CALET on the International Space Station

Shoko Miyake,[a,*] **Kazuoki Munakata**[b] **and Yosui Akaike**[c,d] **for the CALET collaboration**

[a] *National Institute of Technology (KOSEN), Ibaraki College, Department of Industrial Engineering, 866 Nakane, Hitachinaka, Ibaraki 312-8508, Japan*

[b] *Shinshu University, Faculty of Science, 3-1-1 Asahi, Matsumoto, Nagano 390-8621, Japan*

[c] *Waseda University, Waseda Research Institute for Science and Engineering, 17 Kikuicho, Shinjuku, Tokyo 162-0044, Japan*

[d] *Japan Aerospace Exploration Agency, EM Utilization Center, Human Spaceflight Technology Directorate, 2-1-1 Sengen, Tsukuba, Ibaraki 305-8505, Japan*

E-mail: miyakesk@ee.ibaraki-ct.ac.jp, kmuna00@shinshu-u.ac.jp, yakaike@aoni.waseda.jp

We present the solar modulation of electrons and protons observed by the CALorimetric Electron Telescope onboard the International Space Station for about 7 years since October 2015, during the transition phase from the descending phase of the 24th solar cycle to the ascending phase of the 25th solar cycle. The observed variations of electron and proton count rates at an identical average rigidity of 3.8 GV show a clear charge-sign dependence of the solar modulation of galactic cosmic rays (GCRs), which is consistent with the prediction of a numerical drift model of the GCR transport in the heliosphere. It is also found that the ratio of 3.8 GV proton count rate to the neutron monitor count rate in the ascending phase of solar cycle 25 is clearly different from that in the descending phase of cycle 24. Correlations between the electron (proton) count rate and the heliospheric environmental parameters, such as the current sheet tilt angle, are a useful tool in further developing a numerical model of solar modulation.

38th International Cosmic Ray Conference (ICRC2023)
26 July - 3 August, 2023
Nagoya, Japan

ICRC2023
38th International Cosmic Ray Conference
The Astroparticle Physics Conference

*Speaker

PoS(ICRC2023)1253

1. Introduction

The CALorimetric Electron Telescope (CALET) on the International Space Station (ISS) has been measuring high-energy cosmic rays (CRs) and gamma rays to understand the cosmic-ray acceleration and propagation. The CALET also operates in the low-energy electron (LEE) trigger mode at high geomagnetic latitudes that can measure the low-energy CR electrons in the energy region from 1 GeV to 10 GeV, in addition to the high energy (HE) trigger with an energy threshold of 10 GeV. Using this LEE trigger mode, the CALET has observed the charge-sign dependent modulation in an agreement with the prediction of a numerical drift model of the low-energy CR transport in the heliosphere. In this study, we analyze the CR modulation of low-energy electrons and protons observed by CALET for about 7 years since October 2015, during the transition phase from the descending phase of the 24th solar cycle to the ascending phase of the 25th solar cycle.

2. CALET Instrument

The CALET calorimeter consists of a charge detector (CHD) for identifying the charge of the incident particle, an imaging calorimeter (IMC) for track reconstruction and for fine-spatial resolution imaging of the early stage shower development, and a total absorption calorimeter (TASC) for measuring the energy of the electromagnetic and hadronic showers [1]. The CHD is composed of a pair of x-y layers each consisting of 14 plastic scintillator paddles with dimensions of 450 mm long × 32 mm wide × 10 mm thick. The IMC is composed of eight x-y layers of 448 mm long × 1 mm^2 square cross section scintillating fibers interleaved with tungsten plates. The first five tungsten plates have 0.2 radiation length (X_0) thickness and the last two plates each have $1.0X_0$ thickness. The total thickness of the IMC is equivalent to $3X_0$. The TASC consists of twelve crossed layers of 16 lead tungstate logs each with dimensions of 326 mm long × 19 mm wide × 20 mm thick, with total thickness of $27X_0$. The total thickness of the calorimeter is 30 X_0, equivalent to ∼1.3 proton interaction lengths, allowing CALET to obtain nearly total absorption of electron showers even in the TeV energy range.

3. Data Analysis

We analyze the flight data collected in the LEE trigger mode during 2757 days from October 13, 2015 to April 30, 2023. We have collected about 124 million low-energy GCR candidates in a total observational live time of approximately 1044 hours. From this data set, we select electrons and protons and deduce their count rates at the same average rigidity.

For the event selection and energy reconstruction, we refer to Monte Carlo (MC) simulations developed to simulate physical processes and detector response based on the simulation package EPICS [2] (EPICS 9.20 and COSMOS 8.00) and the DPMJET-III model for the hadron interaction. The MC event samples consist of downward propagating electron and proton events generated isotropically on a spherical surface with a radius of 78 cm surrounding the instrument. We apply the following event-selection criteria: (a) off-line trigger condition requiring energy deposits in the bottom two layers of IMC and the top layer of TASC to exceed a given set of thresholds, (b) quality cut on the reconstructed track of incident particle by the Kalman filter method, (c) geometrical

condition requiring the reconstructed track to traverse the CHD top layer and the TASC bottom layer, (d) cut on the CHD output to select incident particles with single charge, (e) cut on an energy deposit in all layers of the IMC and the TASC to exclude events passing through the layer without energy deposit, (f) additional cut on the spatial concentration of hit signals in the IMC bottom layer to reduce the proton contamination for the analysis of electron count rates, and (g) cut on the lateral shower development in the TASC top layer for electron/proton discrimination (see the Supplemental Materials of Adriani et al. [3] about the detail of criteria (f) and (g)). Details of these criteria are provided in [4, 5] for the analysis of high-energy electrons, with the important distinction that the analysis here uses only the IMC bottom layer and TASC top layer for electron/proton discrimination given that the low-energy electrons do not penetrate all layers of the TASC.

In order to minimize the count rate variation due to the cutoff rigidity (COR), we choose periods in which COR is below 0.8 GV and select events recorded with rigidity much higher than the COR. We calculate the COR by back-tracing particle's orbits in the model magnetosphere defined by the IGRF-13 [6] and TS05 [7] empirical models [8]. The COR is calculated for every incident direction of particles reconstructed from the observed data.

For the analysis of the charge-sign dependent solar modulation in this paper, we derive the count rates of electrons and protons at the same average rigidity. The average rigidity of incoming electrons that passed the above selection criteria is estimated to be $\sim$ 3.8 GV referring to the MC results. The average rigidity of the protons is also adjusted to $\sim$ 3.8 GV by limiting the maximum energy deposit in the TASC layers and referring to the MC results. We analyze about 1.03 million electron and 1.71 million proton candidates collected in a total observational live time of about 268 and 269 hours, respectively.

4. Results

Figure 1 shows the electron and proton count rates at an average rigidity of 3.8 GV (blue and red symbols), C_{e^-} and C_p respectively, observed by CALET in each Carrington rotation. The black curve shows the count rate of a neutron monitor at the Oulu station observing $\sim$ 10 GV GCR protons [9, 10], C_{NM}, while the blue and red curves show the electron and proton count rates reproduced by the numerical drift model (see the Supplemental Material of [3] for detail), respectively. In Fig.1, the average count rate from October 2015 to May 2021 is normalized to 100 for comparison with the results presented in Adriani et al. [3]. The most striking feature in Fig. 1 is that the variation amplitude of C_{e^-} is clearly larger than that of C_p at the same average rigidity. This is consistent with the drift model prediction that a stronger anticorrelation between the GCR intensity and the tilt angle of the heliospheric current sheet (HCS) results for $qA < 0$ than for $qA > 0$, where q is the sign of the particle's charge and A is the sign of the solar magnetic field polarity. During periods with $A > 0$, the drift leads electrons ($q < 0$) inward toward the Earth along the HCS, while protons ($q > 0$) arrive at the Earth from the heliospheric polar region with their path lengths, less affected by the HCS waviness. This results in a larger modulation of the electron flux than that of the proton flux at Earth, given the HCS tilt angle varies during periods with $A > 0$. The numerical drift model well reproduces the observed variations in both C_{e^-} and C_p for the descending phase in the 24th solar cycle, though there is room for improvement, especially for a period before 2018. This is clear evidence of the drift effect playing a major role in the long-term GCR modulation.

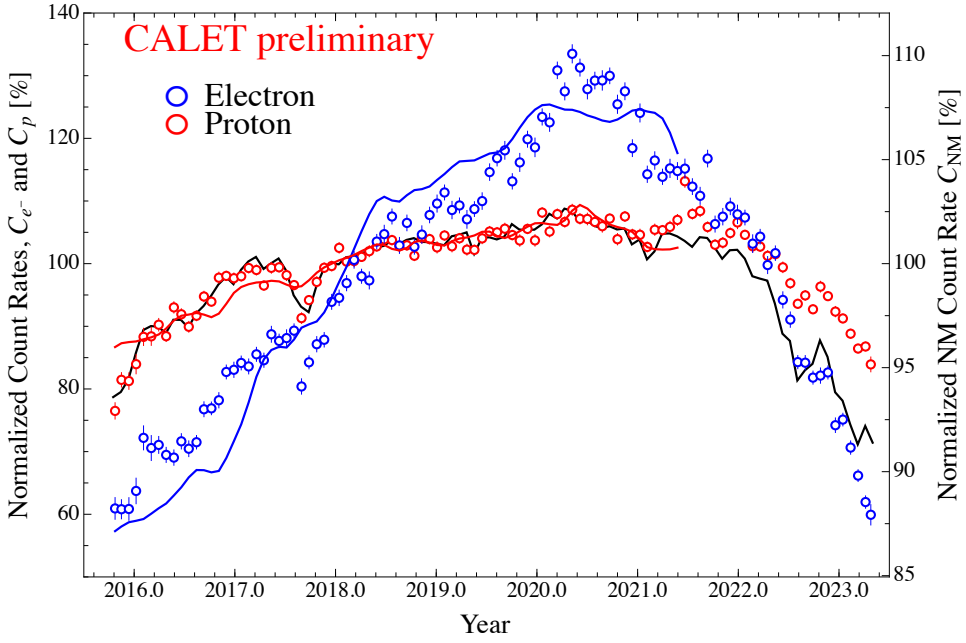

Figure 1: Time profiles of the normalized count rates of electrons C_{e^-} (blue open circles) and protons C_p (red open circles) for each Carrington rotation (left vertical axis), compared with the count rate of a neutron monitor at the Oule station (black curve) on the right vertical axis and the electron (blue curve) and proton (red curve) count rates reproduced by the numerical model.

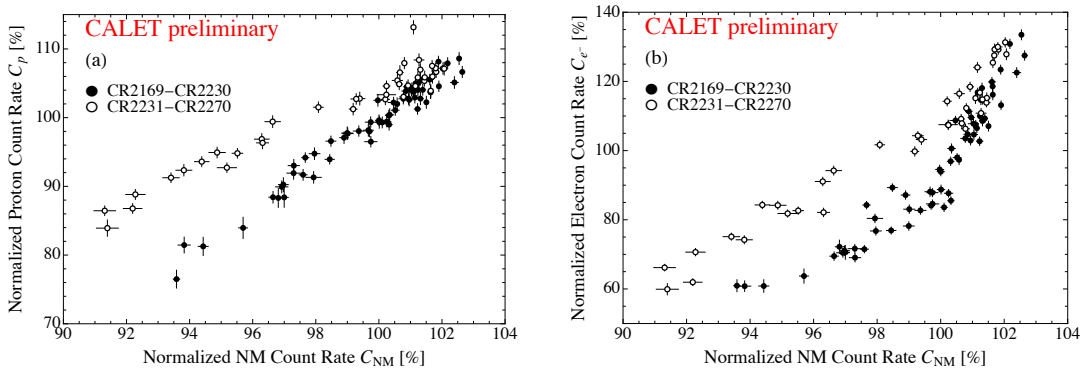

Figure 2: CALET proton (a) and electron (b) count rates at the average rigidity of 3.8 GV as a function of neutron monitor count rates at the Oulu station during the descending phase in the 24th solar cycle (closed circles) and the ascending phase in the 25th solar cycle (open circles).

We also see a good correlation between C_p and $C_{\rm NM}$ in the descending phase in the 24th solar cycle, while the correlation changes in the ascending phases of the 25th solar cycle. This may imply a difference in the rigidity dependence of the solar modulation during the descending and ascending phases. We see in Fig. 2(a) a clear difference between the ratios of C_p to $C_{\rm NM}$ ($C_p/C_{\rm NM}$) during the descending phase of the 24th solar cycle (CR2169~CR2230) and the ascending phase of the 25th solar cycle (CR2231~CR2270). The average ratios ($C_p/C_{\rm NM}$) during the descending phase and the ascending phase are 3.24 and 1.99, respectively, indicating the power-law indices of

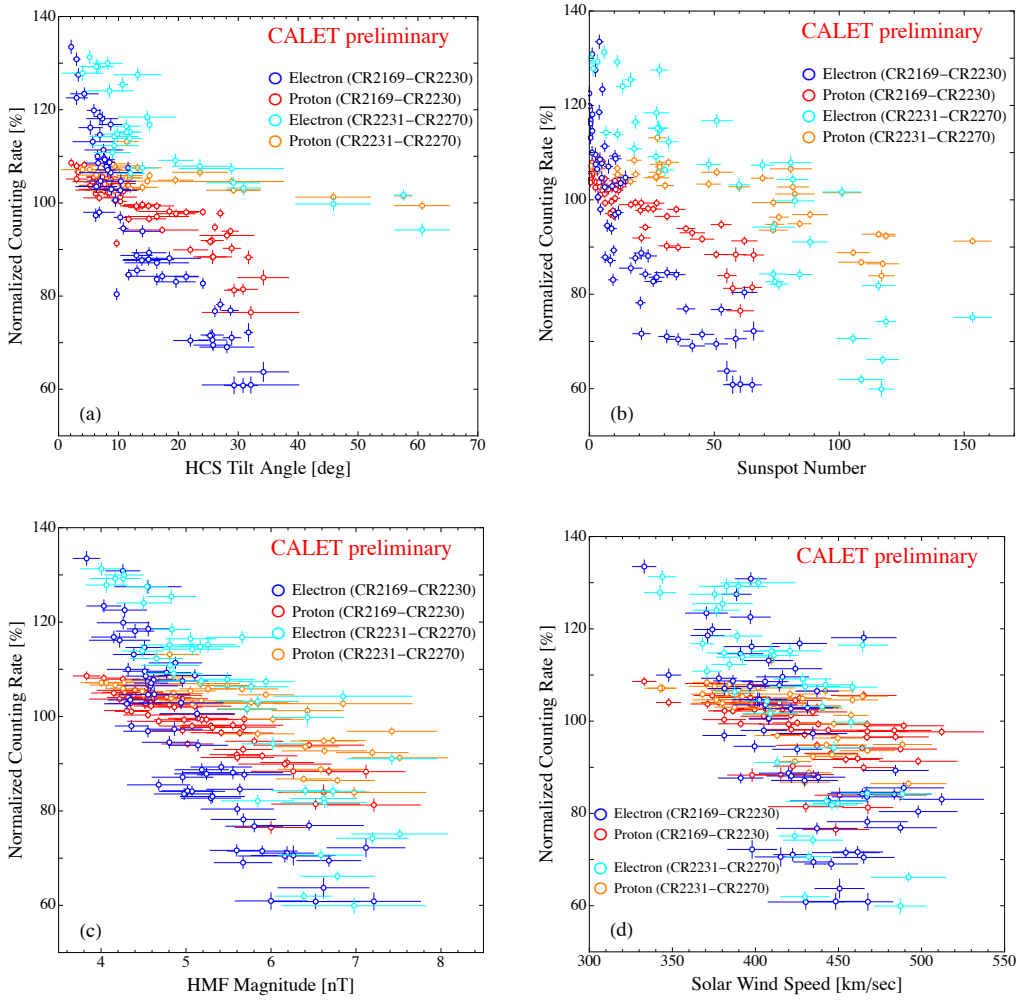

Figure 3: Electron and proton normalized count rates, C_{e^-} and C_p, as a function of the HCS tilt angle (a), the sunspot number (b), the HMF magnitude (c), and the solar wind speed (d). Blue and red open circles show the electron and proton count rates during the descending phase in the 24th solar cycle (CR2169~CR2230) respectively, while cyan and orange open circles show the electron and proton count rates during the ascending phase in the 25th solar cycle (CR2231~CR2270) respectively.

the rigidity spectra of the modulation are -1.21 and -0.71 during the descending and ascending phases, respectively.

Figure 3 shows C_{e^-} (C_p) as a function of the HCS tilt angle (a) [11, 12], the sunspot number (b), the HMF magnitude (c), and the solar wind speed (d) [13]. In Fig. 3(a) and 3(b), we see a hysteresis structure with clockwise rotations of C_{e^-} and C_p. Compared to these figures, there is not a strong hysteresis effect in the correlations with HMF magnitude (Fig. 3(c)) and solar wind speed (Fig. 3(d)). These results strongly support the further development of a numerical model for solar modulation that can better reproduce observations.

5. Conclusion

We have analyzed the normalized count rates of electrons and protons measured by CALET from October 2015 to April 2023. We have obtained a clear charge-sign dependence of the solar modulation of GCRs, showing the variation amplitude of C_{e^-} is much larger than that of C_p at the same average rigidity. We also have succeeded in reproducing variations of C_{e^-} and C_p simultaneously with a numerical drift model of the solar modulation, demonstrating that the drift effect plays a major role in the long-term modulation of GCRs. We also find a clear difference between ratios, $C_p/C_{\rm NM}$, during the descending phase of solar cycle 24 and the ascending phase of solar cycle25. Correlations between C_{e^-} (C_p) and the heliospheric environmental parameters, such as the HCS tilt angle, are clearly important in helping to constrain our numerical model of solar modulation.

Acknowledgments

We gratefully acknowledge JAXA's contributions to the development of CALET and to the operations onboard the International Space Station. The CALET effort in Italy is supported by ASI under Agreement No. 2013-018-R.0 and its amendments. The CALET effort in the United States is supported by NASA through Grants No. 80NSSC20K0397, No. 80NSSC20K0399, and No. NNH18ZDA001N-APRA18-0004. This work is supported in part by JSPS Grant-in-Aid for Scientific Research (S) Grant No. 19H05608, JSPS Grant-in-Aid for Scientific Research (C) Grant No. 20K03956, and JSPS Grant-in-Aid for Scientific Research (C) Grant No. 21K03592 in Japan.

References

[1] Y. Asaoka, Y. Ozawa, S. Torii et al. (CALET Collaboration), Astropart. Phys., **100**, 29 (2018)

[2] K. Kasahara, Proc. of the 24th International Cosmic Ray Conference, Rome, Italy, **1**, 399 (1995)

[3] O. Adriani et al. (CALET Collaboration), Phys. Rev. Lett., **130**, 211001 (2023)

[4] O. Adriani et al. (CALET Collaboration), Phys. Rev. Lett., **119**, 181101 (2017)

[5] O. Adriani et al. (CALET Collaboration), Phys. Rev. Lett., **120**, 261102 (2018)

[6] P. Alken, E. Thébault, C. D. Beggan, H. Amit, J. Aubert et al., Earth Planets Space, **73**, 49 (2021)

[7] N. A. Tsyganenko and M. I. Sitnov, J. Geophys. Res., **110**, A03208 (2005)

[8] S. Miyake, R. Kataoka, and T. Sato, Spece Weather, **15**, 589-605 (2017)

[9] I. G. Usoskin, K. Mursula, J. Kangas, and B. Gvozdevsky, Proceedings of the 27th International Cosmic Ray Conference 2001, Hamburg, Germany, 3842 (2001)

[10] Sodankyla Geophysical Observatory, Oule Cosmic Ray Station, https://cosmicrays.oulu.fi/

[11] J. T. Hoeksema, Space Sci. Rev., **72**, 137-148 (1995)

[12] The Wilcox Solar Observatory, HCS tilt angle, http://wso.stanford.edu/Tilts.html

[13] NASA/Goddard Space Flight Center, OMNIweb, https://omniweb.gsfc.nasa.gov/form/dx1.html

Full Author List: CALET Collaboration

O. Adriani[1,2], Y. Akaike[3,4], K. Asano[5], Y. Asaoka[5], E. Berti[2,6], G. Bigongiari[7,8], W.R. Binns[9], M. Bongi[1,2], P. Brogi[7,8], A. Bruno[10], N. Cannady[11,12,13], G. Castellini[6], C. Checchia[7,8], M.L. Cherry[14], G. Collazuol[15,16], G.A. de Nolfo[10], K. Ebisawa[17], A.W. Ficklin[14], H. Fuke[17], S. Gonzi[1,2,6], T.G. Guzik[14], T. Hams[11], K. Hibino[18], M. Ichimura[19], K. Ioka[20], W. Ishizaki[5], M.H. Israel[9], K. Kasahara[21], J. Kataoka[22], R. Kataoka[23], Y. Katayose[24], C. Kato[25], N. Kawanaka[20], Y. Kawakubo[14], K. Kobayashi[3,4], K. Kohri[26], H.S. Krawczynski[9], J.F. Krizmanic[12], P. Maestro[7,8], P.S. Marrocchesi[7,8], A.M. Messineo[8,27], J.W. Mitchell[12], S. Miyake[28], A.A. Moiseev[29,12,13], M. Mori[30], N. Mori[2], H.M. Motz[18], K. Munakata[25], S. Nakahira[17], J. Nishimura[17], S. Okuno[18], J.F. Ormes[31], S. Ozawa[32], L. Pacini[2,6], P. Papini[2], B.F. Rauch[9], S.B. Ricciarini[2,6], K. Sakai[11,12,13], T. Sakamoto[33], M. Sasaki[29,12,13], Y. Shimizu[18], A. Shiomi[34], P. Spillantini[1], F. Stolzi[7,8], S. Sugita[33], A. Sulaj[7,8], M. Takita[5], T. Tamura[18], T. Terasawa[5], S. Torii[3], Y. Tsunesada[35,36], Y. Uchihori[37], E. Vannuccini[2], J.P. Wefel[14], K. Yamaoka[38], S. Yanagita[39], A. Yoshida[33], K. Yoshida[21], and W.V. Zober[9]

[1]Department of Physics, University of Florence, Via Sansone, 1 - 50019, Sesto Fiorentino, Italy, [2]INFN Sezione di Firenze, Via Sansone, 1 - 50019, Sesto Fiorentino, Italy, [3]Waseda Research Institute for Science and Engineering, Waseda University, 17 Kikuicho, Shinjuku, Tokyo 162-0044, Japan, [4]JEM Utilization Center, Human Spaceflight Technology Directorate, Japan Aerospace Exploration Agency, 2-1-1 Sengen, Tsukuba, Ibaraki 305-8505, Japan, [5]Institute for Cosmic Ray Research, The University of Tokyo, 5-1-5 Kashiwa-no-Ha, Kashiwa, Chiba 277-8582, Japan, [6]Institute of Applied Physics (IFAC), National Research Council (CNR), Via Madonna del Piano, 10, 50019, Sesto Fiorentino, Italy, [7]Department of Physical Sciences, Earth and Environment, University of Siena, via Roma 56, 53100 Siena, Italy, [8]INFN Sezione di Pisa, Polo Fibonacci, Largo B. Pontecorvo, 3 - 56127 Pisa, Italy, [9]Department of Physics and McDonnell Center for the Space Sciences, Washington University, One Brookings Drive, St. Louis, Missouri 63130-4899, USA, [10]Heliospheric Physics Laboratory, NASA/GSFC, Greenbelt, Maryland 20771, USA, [11]Center for Space Sciences and Technology, University of Maryland, Baltimore County, 1000 Hilltop Circle, Baltimore, Maryland 21250, USA, [12]Astroparticle Physics Laboratory, NASA/GSFC, Greenbelt, Maryland 20771, USA, [13]Center for Research and Exploration in Space Sciences and Technology, NASA/GSFC, Greenbelt, Maryland 20771, USA, [14]Department of Physics and Astronomy, Louisiana State University, 202 Nicholson Hall, Baton Rouge, Louisiana 70803, USA, [15]Department of Physics and Astronomy, University of Padova, Via Marzolo, 8, 35131 Padova, Italy, [16]INFN Sezione di Padova, Via Marzolo, 8, 35131 Padova, Italy, [17]Institute of Space and Astronautical Science, Japan Aerospace Exploration Agency, 3-1-1 Yoshinodai, Chuo, Sagamihara, Kanagawa 252-5210, Japan, [18]Kanagawa University, 3-27-1 Rokkakubashi, Kanagawa, Yokohama, Kanagawa 221-8686, Japan, [19]Faculty of Science and Technology, Graduate School of Science and Technology, Hirosaki University, 3, Bunkyo, Hirosaki, Aomori 036-8561, Japan, [20]Yukawa Institute for Theoretical Physics, Kyoto University, Kitashirakawa Oiwake-cho, Sakyo-ku, Kyoto, 606-8502, Japan, [21]Department of Electronic Information Systems, Shibaura Institute of Technology, 307 Fukasaku, Minuma, Saitama 337-8570, Japan, [22]School of Advanced Science and Engineering, Waseda University, 3-4-1 Okubo, Shinjuku, Tokyo 169-8555, Japan, [23]National Institute of Polar Research, 10-3, Midori-cho, Tachikawa, Tokyo 190-8518, Japan, [24]Faculty of Engineering, Division of Intelligent Systems Engineering, Yokohama National University, 79-5 Tokiwadai, Hodogaya, Yokohama 240-8501, Japan, [25]Faculty of Science, Shinshu University, 3-1-1 Asahi, Matsumoto, Nagano 390-8621, Japan, [26]Institute of Particle and Nuclear Studies, High Energy Accelerator Research Organization, 1-1 Oho, Tsukuba, Ibaraki, 305-0801, Japan, [27]University of Pisa, Polo Fibonacci, Largo B. Pontecorvo, 3 - 56127 Pisa, Italy, [28]Department of Electrical and Electronic Systems Engineering, National Institute of Technology (KOSEN), Ibaraki College, 866 Nakane, Hitachinaka, Ibaraki 312-8508, Japan, [29]Department of Astronomy, University of Maryland, College Park, Maryland 20742, USA, [30]Department of Physical Sciences, College of Science and Engineering, Ritsumeikan University, Shiga 525-8577, Japan, [31]Department of Physics and Astronomy, University of Denver, Physics Building, Room 211, 2112 East Wesley Avenue, Denver, Colorado 80208-6900, USA, [32]Quantum ICT Advanced Development Center, National Institute of Information and Communications Technology, 4-2-1 Nukui-Kitamachi, Koganei, Tokyo 184-8795, Japan, [33]College of Science and Engineering, Department of Physics and Mathematics, Aoyama Gakuin University, 5-10-1 Fuchinobe, Chuo, Sagamihara, Kanagawa 252-5258, Japan, [34]College of Industrial Technology, Nihon University, 1-2-1 Izumi, Narashino, Chiba 275-8575, Japan, [35]Graduate School of Science, Osaka Metropolitan University, Sugimoto, Sumiyoshi, Osaka 558-8585, Japan, [36]Nambu Yoichiro Institute for Theoretical and Experimental Physics, Osaka Metropolitan University, Sugimoto, Sumiyoshi, Osaka 558-8585, Japan, [37]National Institutes for Quantum and Radiation Science and Technology, 4-9-1 Anagawa, Inage, Chiba 263-8555, Japan, [38]Nagoya University, Furo, Chikusa, Nagoya 464-8601, Japan, [39]College of Science, Ibaraki University, 2-1-1 Bunkyo, Mito, Ibaraki 310-8512, Japan

PoS(ICRC2023)1253